

CHAPTER 1

Introduction to Surface Plasmon Resonance

ANNA J. TUDOS^a AND RICHARD B.M. SCHASFOORT^b

^a Shell Global Solutions International BV, P.O. Box 38000
1030 BN Amsterdam, The Netherlands; ^b Biochip Group, MESA + Institute
for Nanotechnology, Biomedical Technology Institute (BMTI), Faculty of
Science and Engineering, University of Twente, P.O. Box 217,
7500 AE Enschede, The Netherlands

1.1 What is Surface Plasmon Resonance?

Since its first observation by Wood in 1902 [1,2], the physical phenomenon of surface plasmon resonance (SPR) has found its way into practical applications in sensitive detectors, capable of detecting sub-monomolecular coverage. What is surface plasmon resonance? Wood observed a pattern of “anomalous” dark and light bands in the reflected light, when he shone polarized light on a mirror with a diffraction grating on its surface. Physical interpretation of the phenomenon was initiated by Lord Rayleigh [3], and further refined by Fano [4], but a complete explanation of the phenomenon was not possible until 1968, when Otto [5] and in the same year Kretschmann and Raether [6] reported the excitation of surface plasmons. Application of SPR-based sensors to biomolecular interaction monitoring was first demonstrated in 1983 by Liedberg *et al.* [7]. A historical overview of the use of the phenomenon for biosensor applications is given in Section 1.3 of this chapter. To understand the excitation of surface plasmons, let us start with a simple experiment.

1.1.1 A Simple Experiment

Consider the experimental set-up depicted in Figure 1.1. When polarized light is shone through a prism on a sensor chip with a thin metal film on top, the light will be reflected by the metal film acting as a mirror. On changing the angle of incidence, and monitoring the intensity of the reflected light, the intensity of the

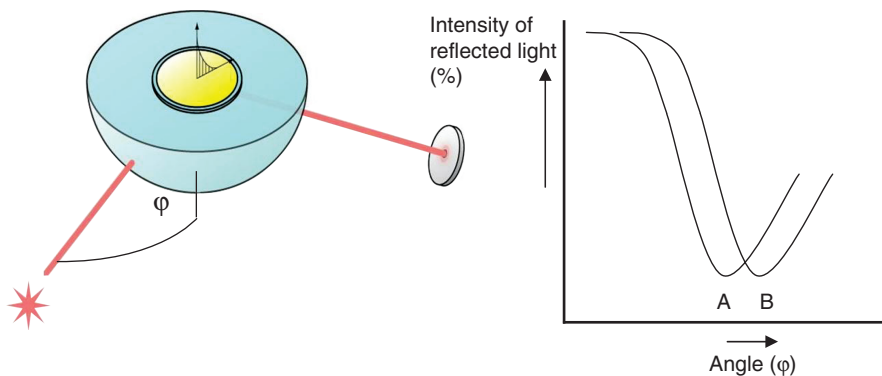


Figure 1.1 Schematic experimental set-up of surface plasmon resonance excitation. A sensor chip with a gold coating is placed on a hemisphere (or prism). Polarized light shines from the light source (star) on the sensor chip. Reflected light intensity is measured in the detector (disk). At a certain angle of incidence (φ), excitation of surface plasmons occurs, resulting in a dip in the intensity of the reflected light (A). A change in refractive index at the surface of the gold film will cause an angle shift from A to B.

reflected light passes through a minimum (Figure 1.1, line A). At this angle of incidence, the light will excite surface plasmons, inducing surface plasmon resonance, causing a dip in the intensity of the reflected light. Photons of p-polarized light can interact with the free electrons of the metal layer, inducing a wave-like oscillation of the free electrons and thereby reducing the reflected light intensity.

The angle at which the maximum loss of the reflected light intensity occurs is called resonance angle or SPR angle. The SPR angle is dependent on the optical characteristics of the system, *e.g.* on the refractive indices of the media at both sides of the metal, usually gold. While the refractive index at the prism side is not changing, the refractive index in the immediate vicinity of the metal surface will change when accumulated mass (*e.g.* proteins) adsorb on it. Hence the surface plasmon resonance conditions are changing and the shift of the SPR angle is suited to provide information on the kinetics of *e.g.* protein adsorption on the surface.

1.1.2 From Dip to Real-time Measurement

Surface plasmon resonance is an excellent method to monitor changes of the refractive index in the near vicinity of the metal surface. When the refractive index changes, the angle at which the intensity minimum is observed will shift as indicated in Figure 1.2, where (A) depicts the original plot of reflected light intensity *vs.* incident angle and (B) indicates the plot after the change in refractive index. Surface plasmon resonance is not only suited to measure the difference between these two states, but can also monitor the change in time, if one follows in time the shift of the resonance angle at which the dip is observed.

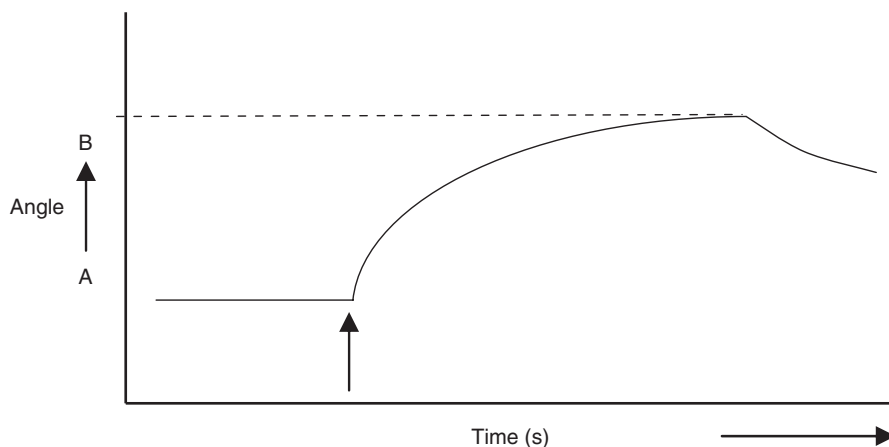


Figure 1.2 A sensorgram: the angle at which the dip is observed *vs.* time. First, no change occurs at the sensor and a baseline is measured with the dip at SPR angle (A). After injection of the sample (arrow) biomolecules will adsorb on the surface resulting in a change in refractive index and a shift of the SPR angle to position B. The adsorption–desorption process can be followed in real time and the amount of adsorbed species can be determined.

Figure 1.2 depicts the shift of the dip in time, a so-called sensorgram. If this change is due to a biomolecular interaction, the kinetics of the interaction can be studied in real time.

SPR sensors investigate only a very limited vicinity or fixed volume at the metal surface. The penetration depth of the electromagnetic field (so-called evanescent field) at which a signal is observed typically does not exceed a few hundred nanometers, decaying exponentially with the distance from the metal layer at the sensor surface. The penetration depth of the evanescent field is a function of the wavelength of the incident light, as explained in Chapter 2.

SPR sensors lack intrinsic selectivity: all refractive index changes in the evanescent field will be reflected in a change of the signal. These changes can be due to refractive index difference of the medium, *e.g.* a change in the buffer composition or concentration; also, adsorption of material on the sensor surface can cause refractive index changes. The amount of adsorbed species can be determined after injection of the original baseline buffer, as shown in Figure 1.2. To permit selective detection at an SPR sensor, its surface needs to be modified with ligands suited for selective capturing of the target compounds but which are not prone to adsorbing any other components present in the sample or buffer media.

1.2 How to Construct an SPR Assay?

Now we have a basic understanding of the surface plasmon resonance signal and how to measure it in time. We know that the sensor surface needs to be modified to allow selective capturing and thus selective measurement of a target compound.

In the following, we are going to learn more about an SPR measurement. First, the steps of an SPR assay will be discussed from immobilization through analysis to regeneration in a measurement cycle. Next, we get acquainted with a typical calibration curve, followed by examples of assay formats. Finally, a short outlook is provided on the basics of the instrumentation.

1.2.1 The Steps of an Assay

In the simplest case of an SPR measurement, a target component or *analyte* is captured by the capturing element or so-called *ligand* (Figure 1.3). The ligand is permanently immobilized on the sensor surface previous to the measurement. Various sensor surfaces with immobilized ligands are commercially available, and many more can be custom-made, as explained in Chapters 6 and 7.

In the simplest case, the event of capturing the analyte by the ligand gives rise to a measurable signal, this is called *direct detection*. Figure 1.4 shows the sensor signal step-by-step in the measurement cycle with direct detection.

Each measurement starts with conditioning the sensor surface with a suitable buffer solution (1). It is of vital relevance to have a reliable baseline before the capturing event starts. At this point, the sensor surface contains the active ligands, ready to capture the target analytes. On injecting the solution containing

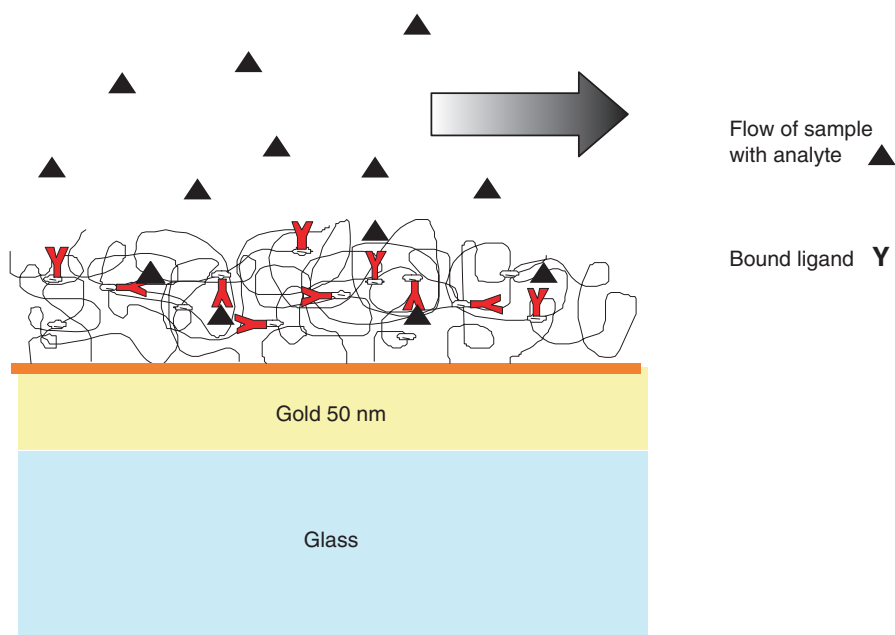


Figure 1.3 Schematic representation of direct detection: the analyte is captured by the ligands (Y) immobilized on the sensor surface. Accumulation of the analyte results in a refractive index change in the evanescent field shifting the SPR angle. Here the ligand is immobilized in a hydrogel.

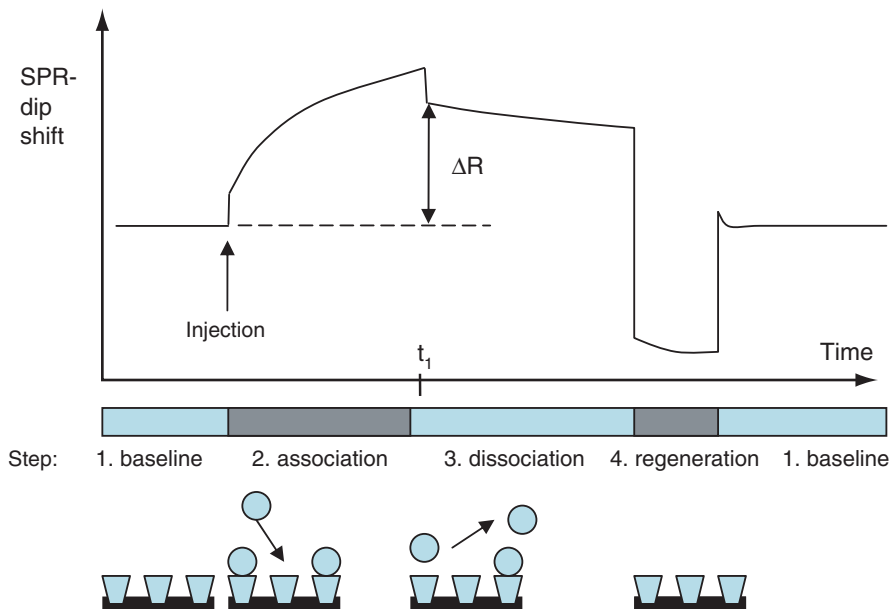


Figure 1.4 Sensorgram showing the steps of an analysis cycle: 1, buffer is in contact with the sensor (baseline step); 2, continuous injection of sample solution (association step); 3, injection of buffer (dissociation step); ΔR indicates the measured response due to the bound target compound; 4, removal of bound species from the surface during injection of regeneration solution (regeneration step) followed by a new analysis cycle. A bulk refractive index shift can be observed at t_1 . See also page 222.

the analytes (2), they are captured on the surface. Also other components of the sample might adhere to the sensor surface; without a suitable selection of the ligand, this adherence will be non-specific, and thus easy to break. At this step, adsorption kinetics of the analyte molecule can be determined in a real-time measurement. Next, buffer is injected on to the sensor and the non-specifically bound components are flushed off (3). As indicated in the figure, the accumulated mass can be obtained from the SPR response (ΔR). Also in this step, dissociation of the analyte starts, enabling the kinetics of the dissociation process to be studied. Finally, a regeneration solution is injected, which breaks the specific binding between analyte and ligand (4). If properly anchored to the sensor surface, the ligands remain on the sensor, whereas the target analytes are quantitatively removed. It is vital in order to perform multiple tests with the same sensor chip to use a regeneration solution which leaves the activity of the ligands intact, as the analysis cycle is required to take place repeatedly for hundreds, sometimes even thousands of times. Again, buffer is injected to condition the surface for the next analysis cycle. If the regeneration is incomplete, remaining accumulated mass causes the baseline level to be increased.

Often SPR measurements are carried out to determine the kinetics of a binding process. For realistic results it is vital to prevent immobilization from

changing the ligand in a way that would influence its strength or affinity towards the target component. In addition, kinetic experiments can provide information on the thermodynamics, *e.g.* on the binding energy of processes. A description of the kinetic theory can be found in Chapter 4 and examples of kinetic studies in Chapter 5.

1.2.2 Calibration Curve

Apart from kinetic and thermodynamic studies, SPR measurements can also be used for the determination of the concentration of the analyte in a sample (quantitative analysis). In this case, first different concentrations of the analyte are applied in separate analysis cycles. The sensorgrams measured at different concentrations give an overlay plot similar to that depicted in Figure 1.5, with the plateaus of the association step increasing at increasing analyte concentration [8].

A calibration curve can be constructed by plotting the response (ΔR) after a certain time interval (t_1) versus concentration.

When analyzing samples with an unknown concentration of the analyte, usually multiple dilutions are made, for example 10, 100 and 1000 times, or for more accurate determinations serial dilutions by a factor of 2. If the concentration

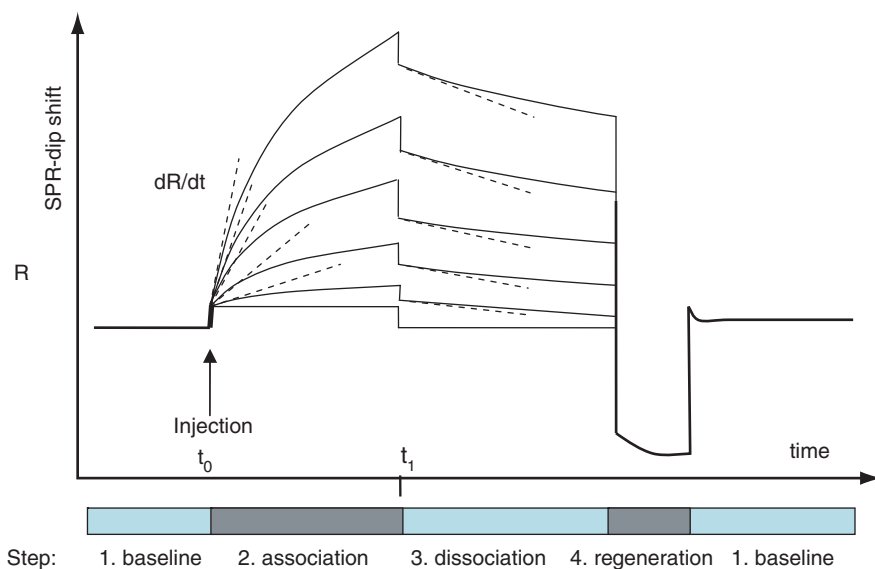


Figure 1.5 Typical overlay plot of sensorgrams from serial diluted analyte concentrations. Just after injection at t_0 a sample specific binding of the analyte occurs and mass transport to the surface is rate limiting and linearly dependent on the concentration. From the slopes of a positive control (dR/dt), the concentration of an unknown sample can be determined. During the association phase the number of unbound ligand molecules decreases and dissociation takes place. The off-rate constant or dissociation constant (k_d) can be determined after injecting dissociation buffer at t_1 . See for more details chapter 4 and 5 of this book.

of the analyte in the sample is very high, the undiluted sample will yield results on the upper plateau range of the calibration curve. The diluted solutions, however, might yield points along the lower, concentration-dependent sections of the calibration curve and the concentration of the analyte can be determined.

As mentioned above, SPR sensing means detection of refractive index changes at the sensor surface, which in practice translates to the amount of mass deposited at the sensor surface. Direct detection is only possible if the capturing event of the analyte brings about measurable refractive index changes. This is easier to achieve if the molecular weight of the analyte is high (*i.e.* around 1000 Da or higher). However, for small molecules to produce a measurable refractive index change, large numbers would be required, making the analysis intrinsically less sensitive. If the analyte is a small molecule (MW < 1000 Da), often direct detection is not viable.

Detection of small molecules can be carried out using a different strategy. Most often, small molecules are detected in a sandwich, competition or inhibition assay format. In all assay formats, not only the lower detectable concentration is limited, but also the physical number of immobilized elements on the sensor surface, which provides a maximum limiting value. Discussion of the different assay formats can be found in Chapter 7 and other methods for concentration determination are described in Chapters 4 and 5.

1.2.3 Determination of Kinetic Parameters

The most prominent benefit of direct detection using SPR biosensor technology is the determination of kinetics of (bio)molecular interactions. Reaction rate and equilibrium constants of interactions can be determined, *e.g.* the interaction $A + B \rightarrow AB$ can be followed in real time with SPR technology, where A is the analyte and B is the ligand immobilized on the sensor surface.

Table 1.1 contains the most relevant kinetic parameters, the association and dissociation constants, for the simplest case $A + B \rightarrow AB$. The association constant is the reaction rate of complex (AB) formation, giving the number of complexes formed per time at unit concentration of A and B. As soon as the complex AB is formed, its dissociation can commence. The dissociation rate constant describing this process expresses the number of AB complexes

Table 1.1 Definitions of the most relevant kinetic parameters: the association and dissociation constants.

	Association rate constant, k_a	Dissociation rate constant, k_d
Definition	$A + B \rightarrow AB$	$AB \rightarrow A + B$
Description	Reaction rate of AB formation: number of AB complexes formed per unit time at unit concentration of A and B	Dissociation rate of AB: number of AB complexes dissociating per unit time
Units	$1 \text{ mol}^{-1} \text{ s}^{-1}$	s^{-1}
Typical range	$10^3\text{--}10^7$	$10^{-1}\text{--}5 \times 10^{-6}$

Table 1.2 Definition of the equilibrium association and dissociation constants.

	<i>Equilibrium association constant, K_A</i>	<i>Equilibrium dissociation constant, K_D</i>
Definition	$[AB]/[A][B] = k_a/k_d$	$[A][B]/[AB] = k_d/k_a$
Description	Affinity to association: high K_A , high affinity to associate	Stability of AB: high K_D , low stability of AB
Unit	1 mol^{-1}	mol l^{-1}
Typical range	10^5 – 10^{12}	10^{-5} – 10^{-12}

dissociating per unit time. Note that the unit dimensions for the association and dissociation rates are different and can vary with the stoichiometry of the complex. The typical range of the association and dissociation constant shows large variations and is dependent on, among other things, the temperature.

When association of A and B starts, no product is yet present at the sensing surface. At this point, the rate of the association reaction is highest and that of the dissociation reaction is lowest. As the process progresses, more and more of the AB complex is produced, enhancing the rate of dissociation. Due to decreasing A and B concentration, the rate of association might decrease. Equilibrium is reached when the rates of the association and dissociation reactions are equal; the definitions and unit dimensions are given in Table 1.2. As can be seen, the equilibrium association and dissociation constants, which represent the affinity of an interaction, have a reciprocal relationship with each other. The effect of parameters such as temperature is described in later chapters.

The rate constants (Table 1.1) and equilibrium constants (Table 1.2) of (bio)molecular interactions provide information on the strength of association and the tendency of dissociation. Various aspects of kinetics, models and calculation of affinity constants are described in Chapters 4, 5 and 9.

1.2.4 Basics of Instrumentation

Studying biomolecular interactions using SPR does not require a detailed understanding of the physical phenomena. It is sufficient to know that SPR-based instruments use an optical method to measure the refractive index near a sensor surface (within ~ 200 nm to the surface). SPR instruments comprise three essential units integrated in one system: optical unit, liquid handling unit and the sensor surface. The features of the sensor chip have a vital influence on the quality of the interaction measurement. The sensor chip forms a physical barrier between the optical unit (dry section) and the flow cell (wet section).

SPR instrumentation can be configured in various ways to measure the shift of the SPR-dip. In general, three different optical systems (Chapter 2) are used to excite surface plasmons: systems with prisms, gratings and optical waveguides. Most widespread are instruments with a prism coupler, also called “Kretschmann configuration” [9]. In this configuration, which is shown in Figure 1.1, a prism couples p-polarized light into the sensor coated with a thin metal film. The light is

reflected on to a detector, measuring its intensity, using a photodiode or a camera. In instruments with a grating coupler [10], light is reflected at the lower refractive index substrate. In practice, this means that light travels through the liquid before photons generate surface plasmon waves as in ellipsometric instruments [11]. Besides the grating couplers, some instruments apply optical waveguide couplers [12] or measure the SPR wavelength shift as a result of the biomolecular interaction process (see Chapter 2 and ref. [13]).

All configurations share the same intrinsic phenomenon: the direct, label-free and real-time measurement of refractive index changes at the sensor surface. SPR sensors offer the capability of measuring low levels of chemical and biological compounds near the sensor surface. Sensing of a biomolecular binding event occurs when biomolecules accumulate at the sensor surface and change the refractive index by replacing the background electrolyte. Protein molecules have a higher refractive index than water molecules ($\Delta n \approx 10^{-1}$). The sensitivity of most SPR instruments is in the range $\Delta n \approx 10^{-5}$ or 1 pg mm^{-2} of proteinous material. Often in real-time biosensing absolute values are not a prerequisite, only the change is monitored as a result of biospecific interaction at the sensor surface. A detailed description of commercial instruments is given in Chapter 3.

1.3 History of SPR Biosensors

The term biosensor was introduced around 1975, relating to exploiting transducer principles for the direct detection of biomolecules at surfaces. Currently the most prominent example of a biosensor is the glucose sensor, reporting glucose concentration as an electronic signal, *e.g.* based on a selective, enzymatic process. Some argued that all small devices capable of reporting parameters of the human body were biosensors (*e.g.* ion-sensitive field-effect transistors (ISFETs) measuring pH). But then, a thermometer recording fever should also be called biosensor. According to the present definition, in biosensors the recognition element (ligand) of the sensor or the analyte should originate from a biological source.

Biosensors are analytical devices comprised of a biological element (tissue, microorganism, organelle, cell receptor, enzyme, antibody) and a physicochemical transducer. Specific interaction between the target analyte and the biological material produces a physico-chemical change detected by the transducer. The transducer then yields an analog electronic signal proportional to the amount (concentration) of a specific analyte or group of analytes.

1.3.1 Early History of SPR Biosensors

Application of SPR-based sensors to biomolecular interaction monitoring was first demonstrated in 1983 by Lundstrom's pursuit towards physical

methods for label-free, real-time detection of biomolecules [7]. The intrinsic properties of the molecules, *e.g.* mass, refractive index and/or charge distribution [14], were probed using ellipsometry, refractometry, surface plasmon resonance, photothermic detection methods and others. At the National Defense Research Laboratory of Sweden, protein–protein interactions were monitored in real time, label-free, using ellipsometry. Most importantly, the refractive index change at a light-reflecting surface was the operating transducer mechanism. Although successful in the detection of refractive index change due to the binding of biomolecules on optical transducer surfaces, a disadvantage of the ellipsometer is that light passes through the bulk of the sample solution, hence light-absorbing or particle-containing samples cannot easily be measured.

Among other research laboratories in the same period, the University of Twente (The Netherlands) was active in the search for finding new transduction principles for measuring immunochemical reactions at field effect transistor devices (ImmunoFET) [15] and at surfaces with an optical read-out (immunochemical optical biosensor, IMOB). Optical transducer principles [16] including ellipsometry, surface plasmon resonance and interferometric principles (Mach Zehnder) showed promise for direct transduction of the biomolecular binding event. Successful measurements of immunochemical reactions using SPR were carried out as early as in the mid-1980s [17].

Pharmacia Biosensor AB chose SPR as their platform technology for direct sensing of biomolecular interactions. The Kretschmann configuration offered advantages in freedom of design of the liquid handling system. Coming from the higher refractive index medium (the prism), light does not pass through the liquid, but is reflected at the sensor surface covered with a thin metal layer. Gold was chosen as the best inert metal film required for surface plasmon resonance, although from a physical point of view silver provides a better SPR effect (see Chapter 2).

Studies on the surface chemistry led to modification of the gold with a self-assembling layer of long-chain thiols to which a hydrogel could be attached. Carboxylated dextran was immobilized at the surface, which provides a substrate for efficient covalent immobilization of biomolecules, in addition to a favorable environment for most biomolecular interactions. The thickness of the dextran hydrogel of 100 nm is perfectly compatible with the *ca.* 200 nm evanescent field (see Figure 1.3). The reliable production of these high-quality sensor chips was unequivocally the basis for the successful launch of SPR instruments.

Techniques were developed to etch silica to form a casting mold for the manufacture of microfluidic flow channels. Also, development proceeded on optogels for use between the prism in the optical unit of the instrument and the sensor chip. The optogel ensures optical contact with the prism, allowing simple replacement of the sensor chip. These efforts in research and development relied on the combination of three unrelated fields: optics, microfluidics and surface chemistry, and resulted in the successful development of the instrumental concept of biomolecular interaction analysis (BIA).

1.3.2 History of SPR Biosensors After 1990

In 1990, Pharmacia Biosensor AB launched the first commercial SPR product, the Biacore instrument [18]. The instrument was the most advanced, sensitive, accurate, reliable, reproducible direct biosensor technique and SPR became (and still is) the “golden standard” of transducer principles for measuring real-time biomolecular interactions. Since the early 1990s, producers have been struggling to meet the standards set by Biacore. Fisons Instruments¹ [19] made serious attempts to compete with Biacore’s technology; their cuvette-based IAsys instrument uses evanescent field-based technology, essentially not SPR, for the study of biomolecular interactions.

The Biacore 2000 instrument was introduced in 1994 with improved detection and a different flow system so that the sample could interact at four spots on the sensor. Data of the reference spot could be used for signal correction. With the introduction of Biacore 2000 it also became possible to monitor directly interactions of small molecule analytes reacting with immobilized protein ligands [20].

In 1995, the cuvette based SPR system of IBIS Technologies was launched. The instrument was compatible with the Biacore sensor chip. In 1997, the IBIS II, a two-channel cuvette-based SPR instrument with autosampler operation, was introduced [21]. Following the merger with the sensor chip coating company Ssens BV in 1999, the development of an SPR imaging instrument was initiated at IBIS Technologies. In 2007, the development of the IBIS-iSPR instrument, with the scanning angle principle, resulted in the required reliability and accuracy for microarray imaging of multiple biomolecular interactions (> 500). The potency of the instrument is demonstrated in Chapter 7.

Biacore X, a two-spot instrument introduced in 1996, was followed by the Biacore 3000 in 1998. The latter was later extended with recovery tools to improve interfacing with mass spectrometry [22]. Biacore Q was introduced for the food analysis market in 2000 (Chapter 11). Positioned for small molecule analysis and drug discovery, the introduction of the Biacore S51 marked a technology shift in terms of detection, flow cell design and sample capacity: the area of the detected spot was reduced from 1 to 0.01 mm² and the number of spots was increased from four to six. In 2004, a high-end instrument was introduced with four channels each with five sensor spots (Biacore A100). Combining the flow cell of the Biacore S51 instrument and the performance of the four-channel Biacore 3000, this instrument has 20 in-line sensors to monitor biomolecular interactions in the flow cells. The technology is not suitable, however, to image the surface. In Chapter 3, other Biacore instruments (T100 and X100) are described. In order to measure up to 400 interactions simultaneously, in 2005 Biacore acquired the grating coupler SPR system of HTS Biosystems, co-developed with Applied Biosystems (8500 Affinity Analyzer), which was capable of imaging the sensor surface. After restyling, this product (named Flexchip) was launched in 2006 [10].

¹Later Affinity Sensors.

Although it is impossible to describe accurately the history of the developments of the 25 companies producing SPR (related) instruments (see Chapter 3), it is justified to treat the history along the Biacore product line. During the years following the introduction of the first SPR instrument, detection sensitivity has improved by roughly 20-fold. The range of affinity and kinetic data that can be determined has been extended at least 100-fold as a consequence of the increased sensitivity and due to improvements in data analysis. The amount of independent sensor surfaces grew from four channels in 1990 (Biacore) to at least 500 in the new IBIS SPR imaging instrument. The carboxymethylated dextran surface introduced in 1990 [23], still the first choice for many applications, has been complemented with a range of other surfaces. Systems for dedicated applications have been introduced by various manufacturers as complements to all-purpose research instrumentation [24]. A good gauge of the success of biosensor technology is that more than 1000 publications each year include data collected from commercial biosensors. In the paper entitled “Survey of the 2005 commercial optical biosensor literature”, Rich and Myszka [25] gave an outstanding overview of the SPR literature, including practical lessons in performing and interpreting biomolecular interaction analysis experiments. The majority of the publications (985) in 2005 employed Biacore technology (87%), indicating the relevance of Biacore’s technology in the market. Affinity Sensors was the runner-up company with 40 publications (~4%), Eco Chemie/Windsor Scientific (distributor) totaled 18 publications, which was essentially from the same technology provider (originally IBIS Technologies), Texas Instruments scored 17 publications in 2005 and 60 publications (~6%) were attributed to 13 other companies.

With the introduction of a number of new SPR instruments (Chapter 3) and a series of novel sensor surfaces and chemistries, the impact of SPR biosensors on molecular interaction studies will continue to grow. With improved experimental design, including SPR imaging instruments and advanced data analysis methods, high-quality data for the determination of kinetic parameters of biomolecular interaction phenomena can be obtained. These data promise additional insights into the mechanisms of molecular binding events, which will be important for function–regulatory protein interaction studies in order to unravel the exciting processes in living species.

1.4 How to Read This Book

Although most chapters can be read as stand-alone literature on different aspects of SPR technology, this handbook aims to provide the reader with a total coverage of the basics of the technique and applications and the most relevant developments at the time of reviewing. The book starts with a description of the physics of surface plasmons and SPR in its original form and some novel applications, for example, nanoparticle SPR.

The description of SPR instrumentation and a survey of currently available commercial products from 25 companies follows in Chapter 3. An introduction on how to obtain kinetic information from SPR measurements can be found in

Chapter 4, followed by Chapter 5 illustrating kinetic and thermodynamic analysis of ligand–receptor interactions, probing the validity of this approach in pharmaceutical applications. Chapter 6 brings the reader closer to the surface architecture and chemical design strategies of SPR sensors. An in-depth treatise on the analysis cycle and modern assay architecture, including SPR microarray imaging, is provided in Chapter 7, followed by advanced methods for SPR imaging biosensing in Chapter 8.

Specific application areas are highlighted in the last few chapters of the book, revealing Surface Plasmon Fluorescence Techniques (Chapter 9) and the future of medical applications at the point of patient care (Chapter 10) and for food safety (Chapter 11). Finally, Chapter 12 gives an outlook on future trends in SPR technology, including “lab-on-a-chip” microfluidics and trends for measuring reliable kinetic parameters.

1.5 Questions

1. SPR technology for direct and label-free detection of biomolecular interactions dominates affinity biosensor technologies to a great extent and it is expected that in 2007 more than 1000 papers regarding SPR results will be published. What are the technical reasons for the success of SPR?
2. In SPR, the intrinsic refractive index of a protein which accumulates on the sensor surface is measured. Explain how we can distinguish between the refractive index of the buffer and that of the adsorbed protein.
3. Why should we express the sensitivity of an SPR instrument in accumulated mass per square surface and not in moles per liter?
4. Consider the monophasic reversible interaction $A + B \rightleftharpoons AB$, where A is the analyte and B is the immobilized ligand. The sample is injected and shows a higher background electrolyte refractive index. Draw the sensorgram of two analysis cycles of injection of a sample with the second analysis cycle a two times diluted sample. Consider 100% regeneration after each analysis cycle.
5. The response ΔR gives us an indication of the amount of accumulated mass per unit surface area. How can we determine the concentration of an analyte in solution from these responses?
6. The study of the rate constants of biomolecular interactions is an important feature of surface plasmon resonance biosensors. Why?

References

1. R.W. Wood, *Philos. Mag.*, 1902, **4**, 396–402.
2. R.W. Wood, *Philos. Mag.*, 1912, **23**, 310–317.
3. Lord Rayleigh, *Proc. R. Soc. London, Ser. A*, 1907, **79**, 399.
4. U. Fano, *J. Opt. Soc. Am.*, 1941, **31**, 213–222.
5. A. Otto, *Z. Phys.*, 1968, **216**, 398–410.

6. E. Kretschmann and H. Reather, *Z. Naturforsch., Teil A*, 1968, **23**, 2135–2136.
7. B. Liedberg, C. Nylander and I. Lundstrom, *Sens. Actuators*, 1983, **4**, 299–304.
8. S. Geib, G. Sandoz, K. Mabrouk, A. Matavel, P. Marchot, T. Hoshi, M. Villaz, M. Ronjat, R. Miquelis, C. Leveque and M. de Waard, *Biochem. J.*, 2002, **364**, 285–292.
9. E. Kretschmann, *Z. Phys.*, 1971, **241**, 313–324.
10. D. Wassaf, G. Kuang, K. Kopacz, Q.L. Wu, Q. Nguyen, M. Toews, J. Cosic, J. Jacques, S. Wiltshire, J. Lambert, C.C. Pazmany, S. Hogan, R.C. Ladner, A.E. Nixon and D.J. Sexton, *Anal. Biochem.*, 2006, **351**, 241–253.
11. M. Pérez-Moralesa, J.M. Pedrosab, E. Muñoz, M.T. Martín-Romeroa, D. Möbiusc and L. Camachoa, *Thin Solid Films*, 2005, **488**, 247–253.
12. J. Ctyroky, J. Homola and M. Skalsky, *Opt. Quantum Electron.*, 1997, **29**, 301–311.
13. C.R. Yonzon, E. Jeoung, S. Zou, G.M. Mrksich and R.P. van Duyne, *J. Am. Chem. Soc.*, 2004, **126**, 12669–12676.
14. Z. Salamon, H.A. Macleod and G. Tollin, *Biochim. Biophys. Acta*, 1997, **1331**, 117–129a.
15. R.B.M. Schasfoort, R.P.H. Kooyman, P. Bergveld and J. Greve, *Biosens. Bioelectron.*, 1990, **5**, 103–125.
16. J. Homola, *Surface Plasmon Resonance Based Sensors*. Springer Series on Chemical Sensors and Biosensors, Series Ed. O.S. Wolfbeis, Vol. 4, Springer, Berlin, 2006.
17. R.P.H. Kooyman, H. Kolkman, J. Van Gent and J. Greve, *Anal. Chim. Acta*, 1988, **213**, 35–45.
18. U. Jonsson, L. Fagerstam, B. Ivarsson, B. Johnsson, R. Karlsson, K. Lundh, S. Lofas, M. Malmqvist, *BioTechniques*, 1991, **11**, 620–622, 624.
19. L.A. Chtcheglova, M. Vogel, H.J. Gruber, G. Dietler and A. Haerberli, *Biopolymers*, 2006, **83**, 69–82.
20. R. Karlsson and R. Stahlberg, *Anal. Biochem.*, 1995, **228**, 274–280.
21. T. Wink, J. de Beer, W.E. Hennink, A. Bult and W.P. van Bennekom, *Anal. Chem.*, 1999, **71**, 801–805.
22. D. Nedelkov, A. Rasooly and R.W. Nelson, *Int. J. Food Microbiol.*, 2000, **60**, 1–13.
23. B. Johnsson, S. Lofas and G. Lindquist, *Anal. Biochem.*, 1991, **198**, 268–277.
24. R.L. Rich and D.G. Myszka, *J. Mol. Recognit.*, 2006, **19**, 478–534.
25. R.L. Rich and D.G. Myszka, *Anal. Biochem.*, 2007, **361**, 1–6.